Worcester Polytechnic Institute
Department of Chemical Engineering

Systematic Synthesis and Characterization of Cellulase Mimetic Polymers

A Major Qualifying Project submitted for review to the faculty of
WORCESTER POLYTECHNIC INSTITUTE

In partial fulfillment of the requirements for the
Degree of Bachelor of Science

Submitted by:
Andrew Wood

Project Advisors:
Dr. Michael Timko, WPI Department of Chemical Engineering
Dr. Marion H. Emmert, WPI Department of Chemistry and Biochemistry

2015

Table of Contents

Abstract

Fossil fuels are not a sustainable fuel source and are a major contributor to global warming. Ethanol produced from biomass, such as corn or wood, has proven to be a good additive to gasoline. This ethanol can be produced from a sustainable resource such as cellulose; unfortunately, current processes towards this goal are expensive and time-consuming.

The herein presented studies seek to systematically synthesize and characterize polymeric catalysts that are functional mimics of cellulose-depolymerizing enzymes, which catalyze the first step (glucose generation) in the production of ethanol from cellulose. The polymeric catalysts under investigation have been proposed to consist of cleaving and binding sites on a polystyrene backbone; the herein presented work is an effort towards establishing a systematic understanding of structure-activity relationships in these materials. To this end, varying polymers have been synthesized. Our investigations provide experimental evidence for the importance of binding sites (C-Cl functionalities) for cellobiose hydrolysis.

Acknowledgements

I want to thank Professors Marion Emmer and Michael Timko for helping and guiding me through every step of this project. I also want to thank Chris Legacy for helping me to improve my writing skills and laboratory skills. Another person I would like to acknowledge is Maksim Tyufekchiev for his collaboration and assistance on some experiments. Finally, I want to thank everyone in Dr. Emmert's lab for providing advice and support throughout the duration of the project.

1. Introduction

1.1 Motivation

The United States consumed 97.53 quadrillion BTU of energy in 2013. Of that, 5% was produced from biomass. [1] Biomass, such as grass or corn, is natural organic material that can be used as a feedstock for fuel. [2] Biofuels, the fuels produced from biomass, are better for the environment than fossil fuels, due to their sustainability and overall lower greenhouse gas (GHG) emissions. [3, 4, 5] Fossil fuels are not sustainable since they are being consumed at a faster rate than they are being produced, whereas biomass can potentially be grown to meet ever-increasing energy demands. [3] CO_2 is produced when fuel is combusted, and it is the main component of GHGs. [6] Plants take in the CO_2 produced during combustion. This production and intake of CO_2 is cyclic. [3] In the case of biofuels, the CO_2 cycle takes a short amount of time to complete, while the cycle for fossil fuels takes millions of years. [7] The use of fossil fuels in transportation is a main contributor to the greenhouse gas effect. [7] The biofuel used most often for transportation is ethanol. [8] Generally, ethanol is used as a non-toxic gasoline additive in order to raise the octane rating. [9] Pure ethanol has a higher engine power output and a better thermal efficiency than gasoline. Due to ethanol's lower vapor pressure, however, it cannot start engines in the cold. [10] In cold climate areas, using ethanol as a fuel requires a 15% gasoline blend in order to solve the cold start issue. [9, 11] This blend has proven to improve engine thermal efficiency and reduce the amount of harmful emissions. [9] To lower the amount of GHG emissions and move toward a more sustainable fuel source, such as ethanol, the US government has mandated that a 140% increase in transportation biofuel consumption must occur by 2022. [6] In order to reach this goal put in place, new developments occur in order to make biofuels a feasible fuel source. [6]

1.2 Biofuels

Biorefineries are production sites that utilize biomass to produce biofuels. First generation use food-based biomasses, which include corn, soy, and sugarcane. [12] These biomasses contain starch, whose chemical structure is shown in Figure 1. [4] Starch consists of glucose monomers linked via α-1, 4 glycosidic bonds. [13] At room temperature, starch molecules form hydrogen bonds, and a helical structure (Figure 2). [14] Upon heating, this helix structure can

be broken, resulting in dissolution of starch; thus, starch can easily reacted to produce glucose with acid catalysts. [15] Subsequently, glucose can be fermented into ethanol.

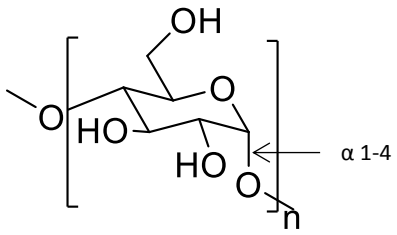

Figure 1: Starch

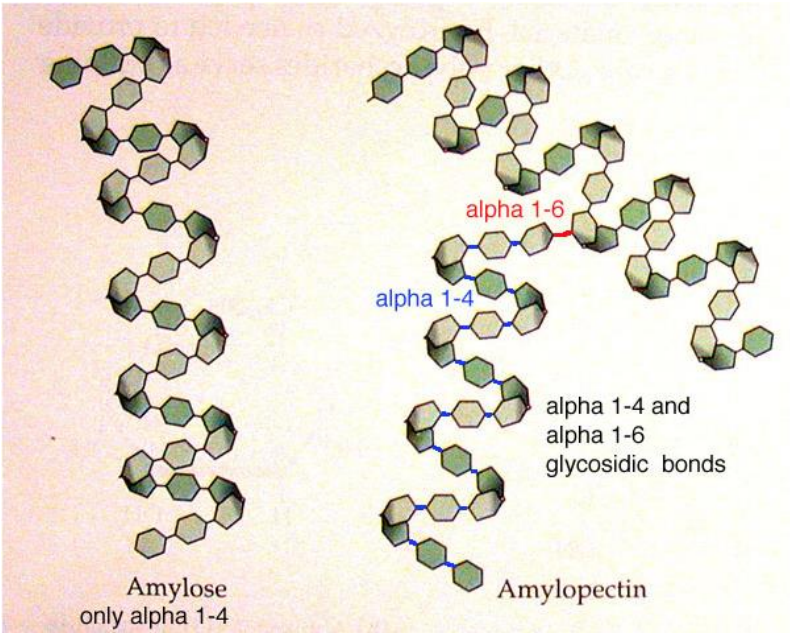

Figure 2: Secondary Structures of Two Forms of Starch [16]

Unfortunately, producing biofuel from sources which can also be used as food resources is not desirable, and cellulosic biomass could be a better option than food based biomass. [17, 18] The US produced 4 billion gallons of ethanol fuel in 2006, and increased to 13.2 billion gallons in 2012 almost solely produced form corn. [17] The government has mandated that 36 billion gallons of ethanol fuel must be produced in 2022. The Renewable Fuel Standard, a government mandated policy, has placed a 15 billion gallon cap on ethanol produced from corn, the

remainder must be produced from cellulosic biomass or biodiesel. This cap was placed on corn based ethanol for many reasons. [13, 18] By producing more corn for biofuels, there is increased land competition with other grains. Also, 40% of the corn grown in the US is used to produce ethanol fuel; only 6% was used to produce ethanol fuel in 2000. This increase has significantly shrunk the percentage of corn used to feed livestock. The price of corn in all sectors has increased around 100% and has created an increase in total food prices. [17, 18] Another issue concerning first generation biofuels is caused by government subsidies. The US government is in debt, but is giving out and estimated $7 billion in subsidies a year to farmers that produce corn for biofuels. [19] Due to these reasons, non-edible biomass would be an overall better option as a fuel feedstock and can solve many of the problems stated above. [18]

Second generation biorefineries produce biofuels from non-edible feedstock such as wood and grasses. 70-95% of non-edible biomass is typically comprised of lignocellulose. Lignocellulosic biomass contains mostly cellulose, some hemicellulose, some lignin, and other minor components. [6] The consistency varies between materials but cellulose is always the main component. [6] Cellulose is the ideal component of this feedstock to be converted to biofuel, since it is the most abundant; furthermore, it is easier to convert to many different biofuels and platform molecules such as ethanol, HMF, and levulinic acid than the other components of lignocellulose. [3] The chemical structure and the secondary structure of cellulose can be seen in Figure 3 and Figure 4. Similar to starch, cellulose is comprised of glucose molecules, which are in this macromolecule linked by β-1, 4 glycosidic bonds. [13] The β-1, 4 glycosidic linkages lead to a 3D structure that enables many hydrogen bonds within each strand and between strands (Figure 4). This causes that formation of a highly crystalline secondary structure. [13] This structure makes cellulose highly resistant dissolution in water and thus more resistant to depolymerization in contrast to starch. [3] In order to convert cellulose into ethanol, the crystallinity must be broken up in order for the β-1, 4 glycosidic bonds to be accessible for hydrolyzation to produce glucose. Without the disruption of the inter- and intra-molecular of cellulose, the catalysts cannot rapidly react with cellulose. [13] Once glucose can be released from cellulose, it can be fermented to produce ethanol in analogy to processes used for first-generation biomass. However, due to the challenging depolymerization and dissolution of cellulose, the cost of ethanol derived from lignocellulose in 2011 was 250-300% higher than the price for ethanol from first generation biorefineries. [20]

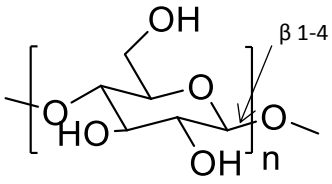

Figure 3: Cellulose

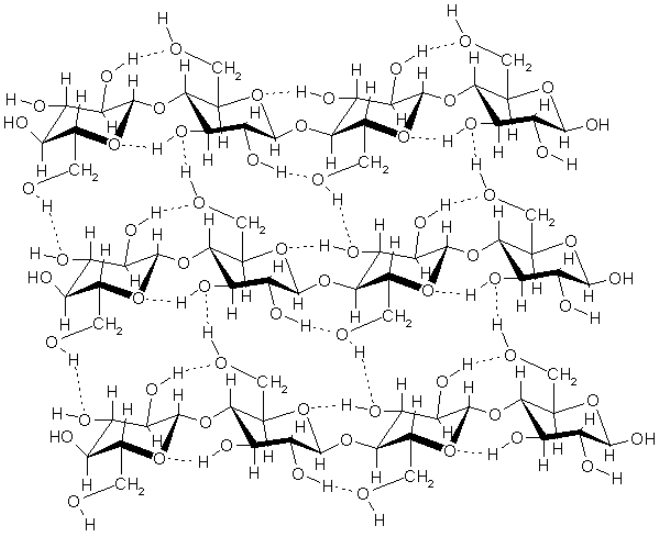

Figure 4: Secondary Structure of Cellulose 16

1.3 Conversion of Cellulose to Glucose

To convert cellulose to ethanol, cellulose needs to undergo hydrolysis into glucose (Figure 5). Hydrolysis is the process of breaking the β-1, 4 glycosidic bonds that bind the glucose moieties in the macromolecules. [3] This process is very difficult due to the crystalline structure and can result in long reaction times, production of undesired chemicals, and thus high costs. The main method of addressing these issues and hydrolyzing cellulose is through the use of enzymes and will be described in detail below. [21]

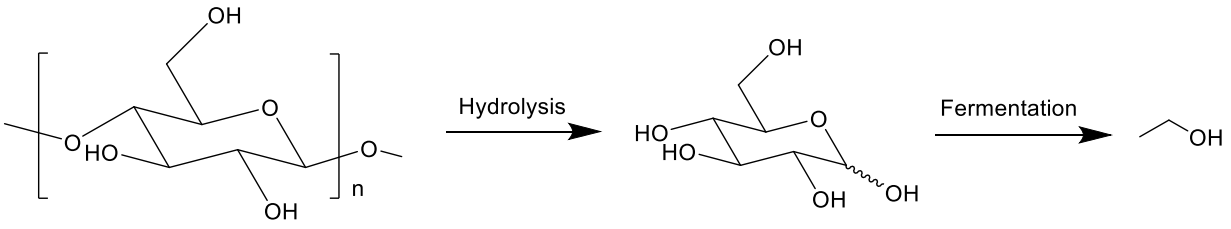

Figure 5: Conversion from Cellulose to Glucose to Ethanol

The enzymes hydrolyze cellulose are known as cellulases. [6] Second generation biorefineries currently use cellulases to generate glucose, and operate at a low temperature, due to the danger of denaturing cellulase at high temperatures. [22] This low heating cost is important in production, since cellulases are very expensive. [6, 20] Cellulase production alone accounts for roughly 40% of the overall cost to produce ethanol from lignocellulosic biomass. [23] Cellulase is expensive since it is produced from different forms of fungi, and also due to competition with paper recycling, cotton, detergent, and food processing industries. [24, 25] Cellulase produces a 70% yield of glucose after one day, and can take six more days to fully hydrolyze cellulose. [3] Due to the long reaction times, cellulases don't seem to be ideal catalysts for hydrolysis and faster, more thermally stable catalysts are highly desirable. [26]

Cellulases are able to hydrolyze cellulose due to their binding and cleaving sites. [26] The hydrolysis mechanism for endoglucanase, a component of cellulase, and cellulose can be seen in Figure 6. The binding sites bind to the hydroxyl groups on cellulose through hydrogen bonds. This disrupts the intra- and inter-molecular bonds of cellulose, which allows the cleaving sites access to the glycosidic bonds. [27] The cleaving site hydrolyzes the glycosidic linkages of the chain into dimers of D-glucose. [26]

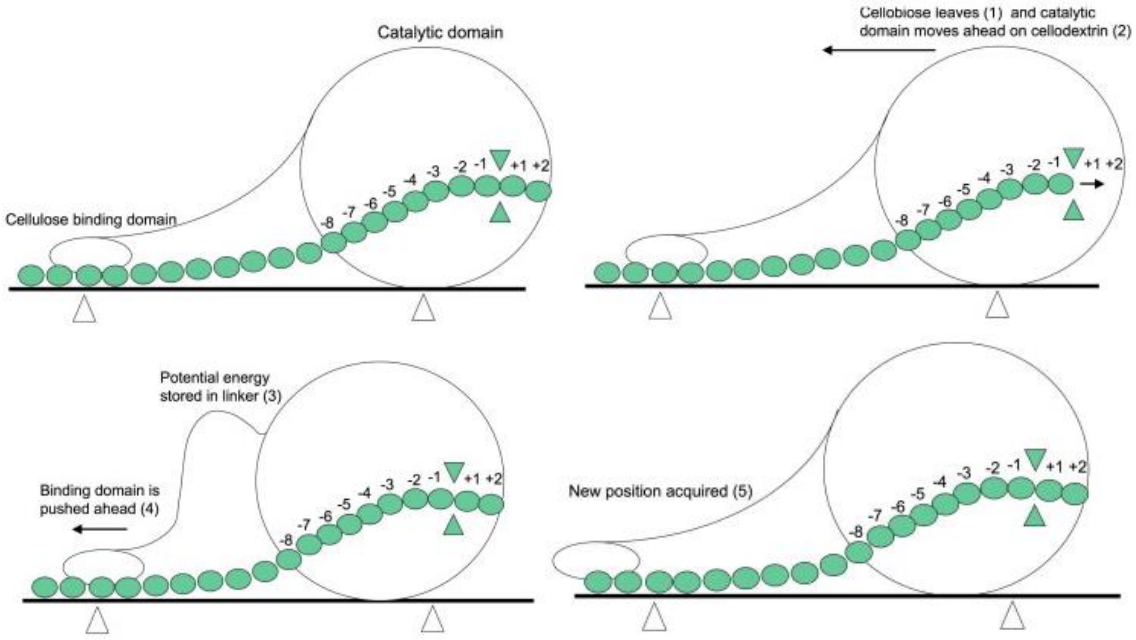

Figure 6: Hydrolysis Mechanism of Endoglucanase Complex and Cellulose 28

1.4 Sulfonated Chloromethyl Polystyrene

A group of researchers from the University of Wisconsin-Madison have created a polymeric catalyst which is inspired by the structure of cellulases. [26, 3] This allegedly cellulase-mimetic catalyst bears benzylchloride moieties as binding sites and sulfonic acid groups mimicking cleaving sites. The catalyst is called sulfonated chloromethyl polystyrene (CP-SO_3H), and its proposed structure is shown in Figure 7; however, the structure of the catalyst has not been fully elucidated by the inventors. The presence of new bonds in CP-SO_3H was determined through Attenuated Total Reflection Fourier Transform Infrared (ATR-FTIR) spectroscopy. [26] The spectra showed that during synthesis, sulfanilic acid replaces some chloride groups. However, this method is qualitative, and did not provide insight into the distribution of sulfonate groups on the surface of the catalyst or the amount of incorporated sulfonyl groups.

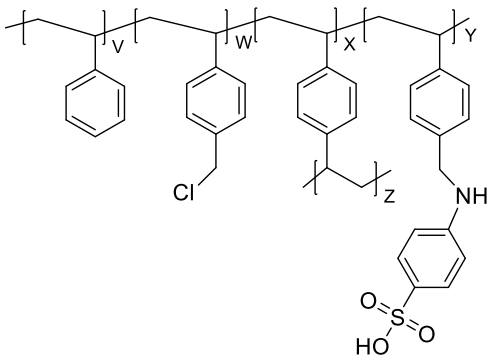

Figure 7: Sulfonated Chloromethyl Polystyrene

The proposed mechanism explains why the CP-SO_3H catalyst can hydrolyze cellulose is because it behaves like cellulase in so far as precoordination between CP-SO_3H and cellulose through hydrogen bonds enables subsequent hydrolysis (

Figure 8). [26, 3] Hydrolysis with the sulfonic acid groups catalyzing cleavage of the glycosidic bonds. [26]

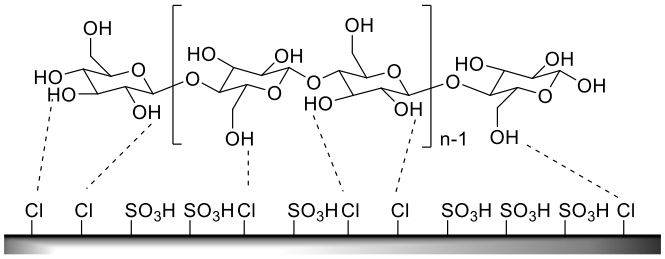

Figure 8: Proposed Precoordination of CP-SO_3H and cellulose

In Shuai and Pan's study of CP-SO_3H, cellobiose was used instead of cellulose. [26] Cellobiose is a dimer of D-glucose units connected via a β-1, 4 glycosidic bond, making it a soluble model system for cellulose. [29] The solid acid polymer is reported to fully hydrolyzed cellobiose into glucose in only two hours. Under the same conditions with identical acid loading, sulfuric acid only hydrolyzed 8% of cellobiose. Sulfuric acid, unlike CP-SO_3H, is completely dissociated in water thus has no binding sites; thus, the authors propose that this is the reason that sulfuric acid did not hydrolyze cellobiose as well as CP-SO_3H. [26] In order for sulfuric acid to completely hydrolyze cellobiose, the temperature, acid loading, and reaction time needed to be increased. In conclusion, CP-SO_3H is a better overall catalyst than sulfuric acid, which is likely due to the chlorine groups forming hydrogen bonds with the cellobiose and thus achieving precoordination of the polymer in proximity to the active acid sites. [26]

Due to the lack of catalyst characterization, however, a good understanding of the catalytic activity and its relationship to the catalyst structure is currently lacking. [26] We propose that determining the structure will provide insight to the reaction mechanism, and will facilitate the development of better catalysts. [26]

1.5 Project Goal

In order to address the gap in the knowledge of structure-activity relationships in the above described catalyst systems, this project will systematically synthesize and characterize different sulfonated chloromethyl polystyrene catalysts. To systematically synthesize different catalysts, the amount of reagent (sulfanilic acid) added to the reaction will vary (Figure 9). By varying the amount of reagent added, it is suspected that there will be different amounts of acid

on the surface of the catalyst. Previous work has only synthesized one catalyst. Two different substrates (chloromethyl polystyrene) will be used, one with twice as much chlorine sites per gram than the other. The synthesized catalysts will also be reacted with cellobiose in order to confirm catalytic activities as documented in the literature, and to see the effect of varied amounts of binding and cleaving sites.

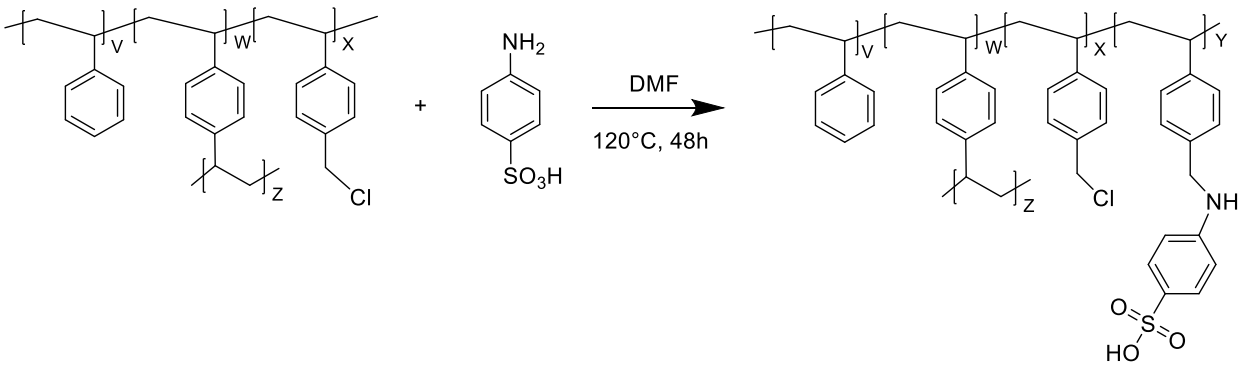

Figure 9: Synthesis of CP-SO_3H

1.6 Significance of the Performed Research

A novel cellulase-mimetic polymer catalyst was produced, and has shown great ability to hydrolyze cellulose; however, not enough data regarding catalyst structure and activity have been collected to begin using this catalyst on large scales yet. [26] The goal of this project is to systematically synthesize and characterize polymeric catalysts related to the described CP-SO3H catalyst. *The following characterization efforts will provide insight into the catalyst's structure its influence on the hydrolysis activity.* This project will aid in the understanding of the catalytic hydrolysis of cellulose. With more knowledge about these types of catalysts, more developments can be made to using lignocellulose as a biomass feedstock.

1.7 Approach

By varying the amount of reagent added during catalyst synthesis, it is suspected that there will be different amounts of binding and cleaving sites on the surface of the catalyst (

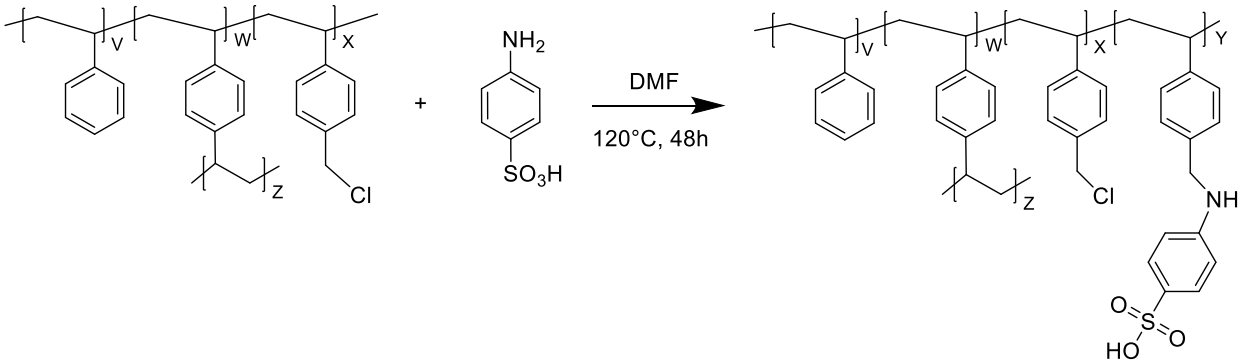

Figure 9). The amount of reagent added will vary from 0.25 equivalents to 10 equivalents. By adding only 0.25 equivalents of reagent, the maximum percentage of chlorine that could be replaced on the polymer is 25%. By adding more than 1 equivalent of reagent, it is possible that all of the chlorine will be replaced. By adding 10 equivalents, the goal is to synthesize a catalyst that only has cleaving sites. The amount of total sites can also be adjusted by using different starting polymers with different amounts of chlorine. For this project, we used two different starting polymers, which will be referred to as low and high site density. The low site density starting polymer has 1.2 mmol of chlorine per gram. The high site density starting polymer has double this amount at 2.4 mmol of chlorine per gram. We predicted that there would be a difference in acid content on the catalysts as well as differneces in the catalytic activity.

To characterize the resulting polymeric catalysts, both qualitative and quantitative methods will be employed. Fourier Transform Infrared (FTIR) spectroscopy will provide a qualitative analysis of components in all polymeric materials. FTIR spectroscopy will show bonds in the substrate as well as in the catalysts. Total Reflection X-Ray Fluorescence (TXRF) will provide a quantitative analysis of the sulfur to chlorine ratio on all catalysts. This will be important to determine what occurs during synthesis, as well as to determine the importance of binding and cleaving sites during hydrolysis.

In order to study the importance of the ratio between binding and cleaving sites on the catalyst, the catalysts will also be reacted with cellobiose to characterize their hydrolytic abilities. The products will be analyzed by high pressure liquid chromatography (HPLC) in order to determine the amount of cellobiose converted to glucose.

2 Results and Discussion

2.1 Synthesis of CP-SO_3H

To produce the CP-SO_3H catalysts, sulfanilic acid is reacted with chloromethyl polystyrene. [26] A schematic representation of the synthesis is shown in

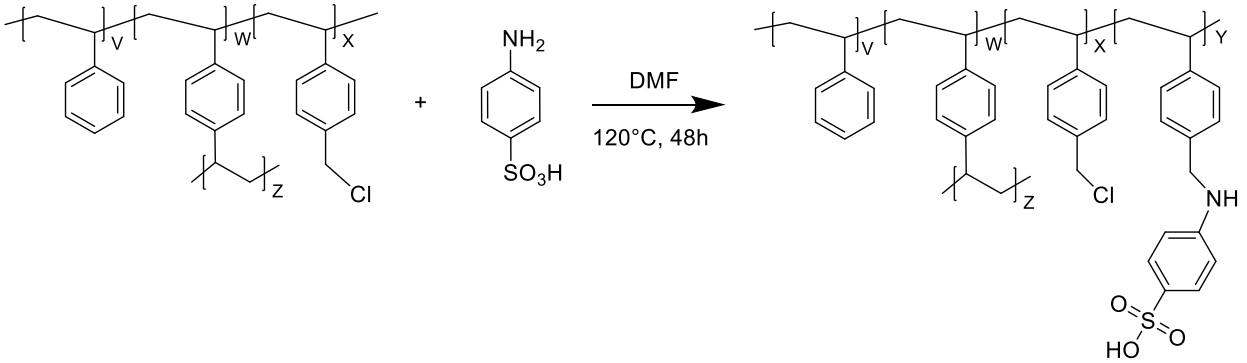

Figure 9. By adding varying equivalents of sulfanilic acid to the reaction, we were hoping to produce catalysts with different acid contents and subsequently varying cleaving to binding site ratios. We had hoped that at a high amount of acid added to the reaction would produce a catalyst devoid of binding sites. Since sulfanilic acid is supposed to replace chlorine during synthesis, it was suspected that the mass of the catalysts would be higher than the mass of the starting material. To test this hypothesis, the mass of the substrate was taken before synthesis, and the mass of the catalyst was taken after filtration and drying. Table 1 shows the amount of substrate and chlorine before synthesis, the equivalents of reagent added to the reaction, and the amount of catalyst produced. Due to transferring and filtration issues, there was always some catalyst loss. The amount of catalyst produced was a promising result, since in general it is higher than the weight of the substrate. Also, generally the amount of catalyst increases with higher equivalents of sulfanilic acid added to the reaction. This result indicated that sulfanilic acid could replace chlorine during synthesis, and that higher acid equivalents yields higher replacement of chlorine. In order to see if higher reagent equivalents yielded higher replacement of chlorine, the catalysts were analyzed using Total X-Ray Fluorescence (TXRF).

Table 1: CP-SO3H Synthesis Results

Entry	Density of Cl in Substrate	Amount of Substrate (g)	Reagent Equivalents	Amount of Catalyst (g)

	(mmol/g)			
2AJW15B	1.2	3	0.25	2.9662
2AJW19B	1.2	3	0.3	2.9029
2AJW9A	1.2	3	0.75	2.994
2AJW13A	1.2	3	1.5	3.067
2AJW9B	1.2	3	2	3.004
2AJW13B	1.2	3	3	3.1206
2AJW19A	1.2	3	4	3.0858
2AJW15A	1.2	3	5	3.1053
2AJW11A	2.4	3	0.75	2.9888
2AJW11B	2.4	3	2	3.0329
2AJW17B	2.4	3	3	3.4782

2.2 Characterization of CP-SO_3H Catalysts

2.2.1 Titration

We predicted that by doing an acid base titration with the catalyst immersed and filtered out of the basic solution, that the amount of acid sites on the catalyst would be quantified. We conducted titrations with a polymer with a known acid content of 5 mmol/g in order to make sure our methods were correct before we titrated the catalysts. Our results showed that the acid content on the polymer was 4.99 mmol/g. Since this value is very close to the real acid content, we began titrating with the synthesized catalysts. After adding catalysts to the base, we noted that the catalysts were very hydrophobic. The hydrophobicity of the catalysts resulted in unrealistic and inconsistent results. Some results showed that there were basic sited on the catalysts, where others showed very little amount of acid. When a titration of the starting polymer (CP resin) was conducted, it showed to have a small acid content. The chlorine is most likely the cause of the result. Since the catalysts also have chlorine, it can be suspected that that causes false results as well. The titrations proved to be a very unreliable characterization method due to the hydrophobicity of the catalysts and the chlorine on the catalysts.

2.2.2 Total Reflection X-Ray Fluorescence (TXRF) Spectroscopy Analysis

Initially, we hoped to use TXRF analysis as a quantitative method to determine the amount of chlorine and sulfur on the starting material as well as on the catalysts. In order to attain quantitative results, a known quantity of a standard must be mixed with the material being analyzed. Both the catalyst and the starting polymer are insoluble in all solvents. Mortar and pestle was used to mix sodium phosphate with the starting polymer or a catalyst. This did not produce a homogenous mixture yielding improper and inconsistent results. Therefore, TXRF analysis could only be fully quantitative.

We were able to produce semi-quantitative results through the use of TXRF analysis. The amount of sulfur can be compared to the amount of chlorine in the catalyst. Since the binding site of the catalyst is proposed to be chlorine and the cleaving site contains sulfur, the ratio of sulfur to chlorine in a catalyst represents the ratio of cleaving to binding sites. Initially, we hypothesized that the ratio of sulfur to chlorine would increase as the amount of reagent added during synthesis increased. Upon very high equivalents of reagent added during synthesis, the sulfur to chlorine ratio was believed to approach infinity, since all of the chlorine would be replaced by sulfanilic acid. Figure 10 shows the sulfur to chlorine ratio in all of the CP-SO_3H catalysts synthesized using a low site density starting material. The high site density catalysts will be described in the next paragraph. The TXRF data shows that until around two equivalents of reagent added the sulfur to chlorine ratio increases linearly. This represents an increase in cleaving sites on the catalysts. The region from two to four reagent equivalents also appears linear, but at a lower slope than from zero to two. This represents more replacement of chlorine during synthesis, but increased hindrance. The sulfur to chlorine ratio reaches a maximum of 2.5 at four equivalents of reagent. This is the catalyst with the highest amount of cleaving sites compared to binding sites. It is not known if this has the highest acid content due to possible side reactions and elements not accounted for in TXRF analysis. When the reagent equivalent is increased further, the sulfur to chlorine ratio begins to decrease. This demonstrates the presence of a side reaction during synthesis. One possibility is the formation of alcohols on the catalysts. Due to an increased amount of sulfanilic acid in the batch, the pH of the solution could rise. The excess hydrogen could interact with the chlorine on the polymer and hydroxide groups from water could replace the chlorine. Another possibility is mixing issues produced from the

increased amount of sulfanilic acid. The solvent becomes oversaturated with an excess of solid sulfanilic acid on the bottom of the batch. Now, with both solid reagent and substrate in the batch, the stir bar may not have produced enough mixing to produce the proper sulfur to chlorine ratios in the catalysts.

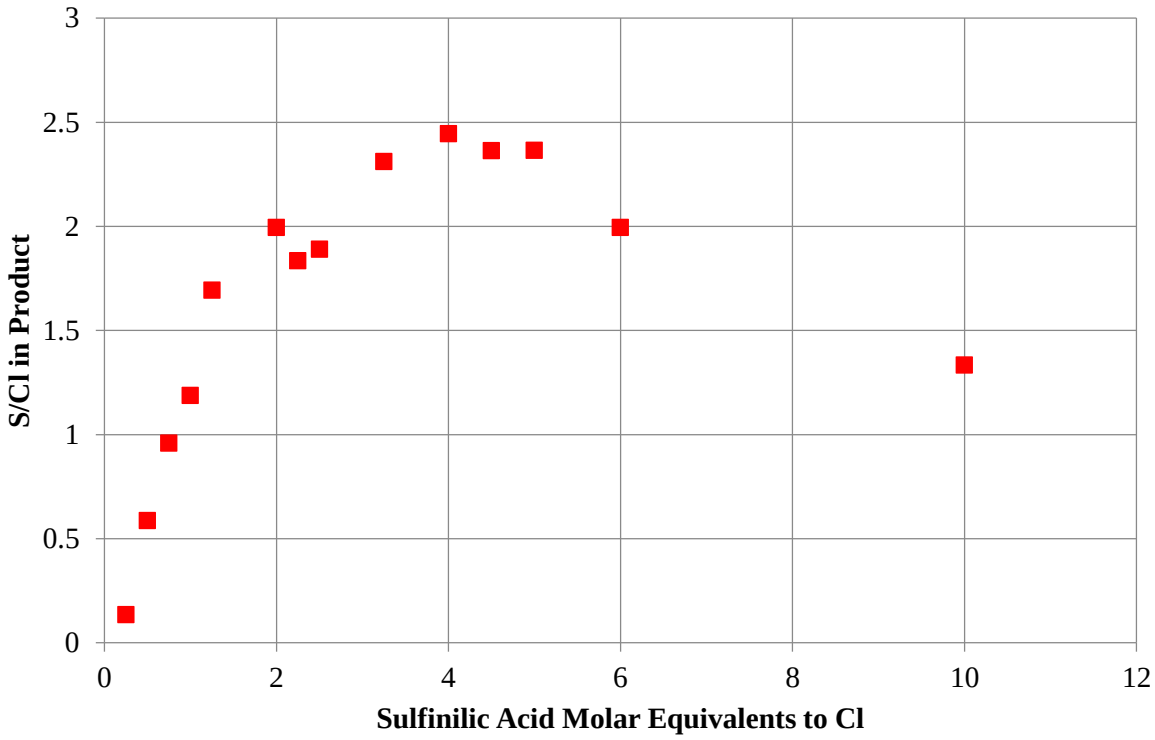

Figure 10: TXRF Data of Sulfur to Chlorine Ratio in Low Site Density Catalysts

We were able to produce semi-quantitative results for the sulfur to chlorine ratio in the high site density catalysts, just like for the low site density catalysts. The sulfur to chlorine ratio was expected to be lower for the high site density resin. This hypothesis is due to the fact that there are more total chlorines on the polymer, which will result in more trapped chlorine not able to be replaced by sulfanilic acid. If side reactions are caused by a high acidity of the solvent, it was expected that the maximum would occur at two equivalents of reagent, since there would be the same amount of acid added to the solution. Figure 11 shows the TXRF data of the high site density catalysts. The trend is not as clear as for the low site density resin, but it appears that the sulfur to chlorine ratio increases until a maximum is reached at two equivalents, and then the

ratio decreases when more acid is added to the synthesis. More syntheses need to be performed in order to determine the reproducibility of the catalysts. Overall, the sulfur to chlorine ratios are all lower in the high site density catalysts as compared to the low site density catalysts. This is most likely due to more chlorine being trapped and not available for replacement. The maximum sulfur to chlorine ratio is reached at two equivalents, which helps confirm the hypothesis that side reactions are occurring due to high acid content in the solvent. The most likely possibility, as stated in the previous paragraph, is the formation of alcohol on the polymer, due to high pH level of the solvent.

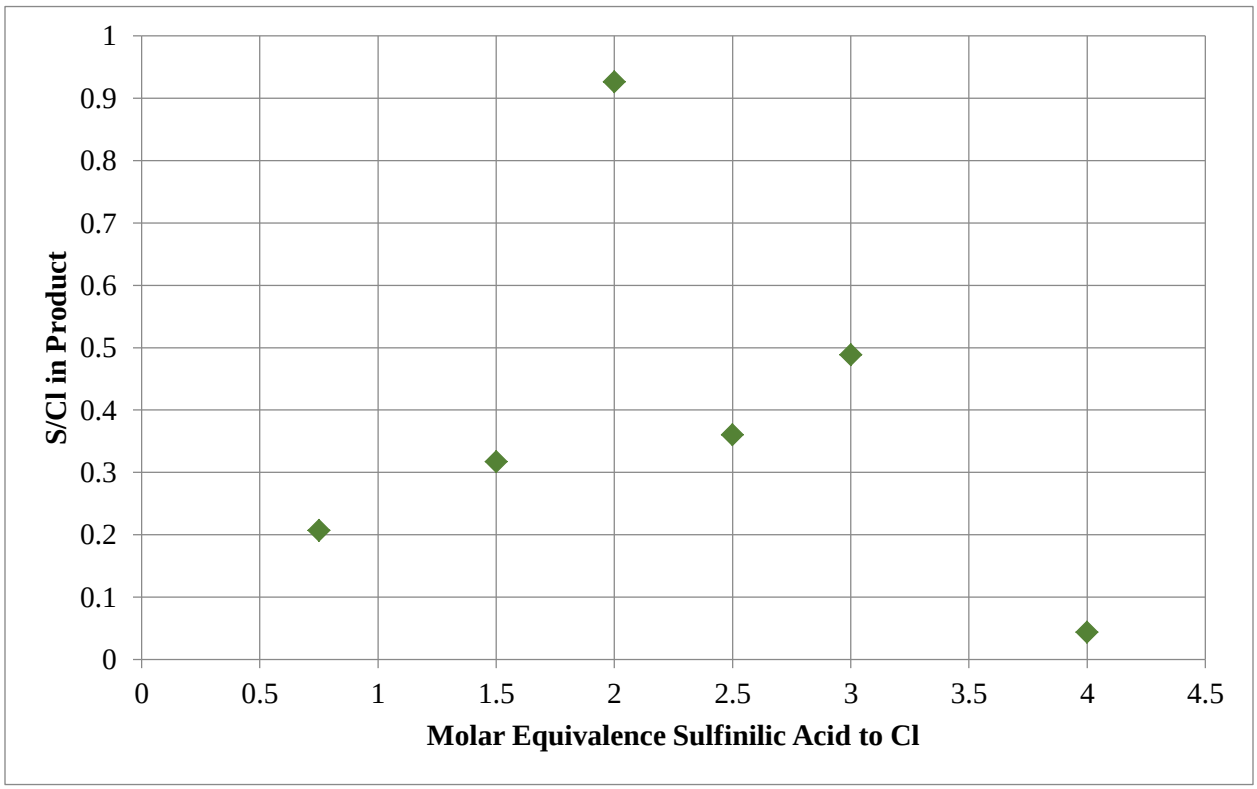

Figure 11: TXRF Data of Sulfur to Chlorine Ratio in High Site Density Catalysts

2.2.3 Fourier Transform Infrared (FTIR) Spectroscopy Analysis

In order to determine the functional groups on all polymeric materials, we used Attenuated Total Reflection (ATR) FTIR spectroscopy. ATR-FTIR is a qualitative analysis method that depends on the quantity of sample being analyzed, as well as the orientation of the

sample during measurement. Both of these issues are uncontrollable due to variations in sample positioning and static charge between the sample and the anvil lowered onto the sample. Although ATR-FTIR cannot provide an exact amount of binding and cleaving groups on the catalyst, it can provide insight to the functional groups on all polymeric materials. We hypothesized that there would be no nitrogen or sulfur groups on the starting material, but we would see them on the catalysts. Based on the TXRF data, we also hypothesized to see functional groups that would indicate side reactions. On ATR-FTIR spectroscopy, unfortunately, the O-H groups that might form resonate at the same wavelength as N-H and it is difficult to tell them apart.

We were able to produce reliable spectra for our catalysts as well as for the CP resin. Figure 12 shows the entire spectra for CP resin and three catalysts. These three catalysts were chosen to show in the report due to their sulfur to chlorine ratios. The catalysts labelled as high and low reagent equivalents have roughly the same S/Cl ratio, but differ in the amount of reagent added during synthesis. The catalyst with the highest S/Cl ratio is shown in red and the S/Cl is about two times greater than that of the other catalysts shown.

As shown in Figure 13, the catalyst spectra have higher intensities at the aromatic carbon region (1615-1580 cm^{-1}) than the CP resin spectrum. The higher intensity in the aromatic carbon region indicates an increase in aromatic carbon after synthesis. One possibility is that sulfanilic acid replaces chlorine. The aromatic ring in the sulfanilic acid would account for the increase in intensity at the aromatic carbon region. The catalyst spectra also show lower intensities at the chlorine region (1280-1260 cm^{-1}) than the CP resin spectrum. This indicates less chlorine in the catalysts than in the starting material. This helps confirm the hypothesis that chlorine is replaced by sulfanilic acid during synthesis. The catalyst spectra also have a stretch around 3400 cm^{-1}. This stretch indicates either N-H or O-H. This stretch cannot be accounted for either but it indicated that the starting material does not have any nitrogen or oxygen. The catalyst spectra also have a sulfonate peak (1120 cm^{-1}) which the CP resin spectrum does not have. This helps confirm that the chlorine in the CP resin is being replaced by sulfanilic acid. The catalyst with the highest S/Cl ratio has the highest intensity at the sulfonate peak and the lowest intensity at the chlorine peak than the other catalysts. This indicated that this catalyst has the least amount of chlorine and the most amount of sulfonate; which confirms the S/Cl ratio found from TXRF

analysis. The catalyst with the highest reagent equivalents has a lower intensity than the other catalysts at the sulfonate peak. This indicates that less sulfonic acid replaced chlorine during synthesis. Overall, the FTIR analysis demonstrates that sulfanilic acid replaces chlorine during synthesis, and that this replacement reaches a maximum at some point.

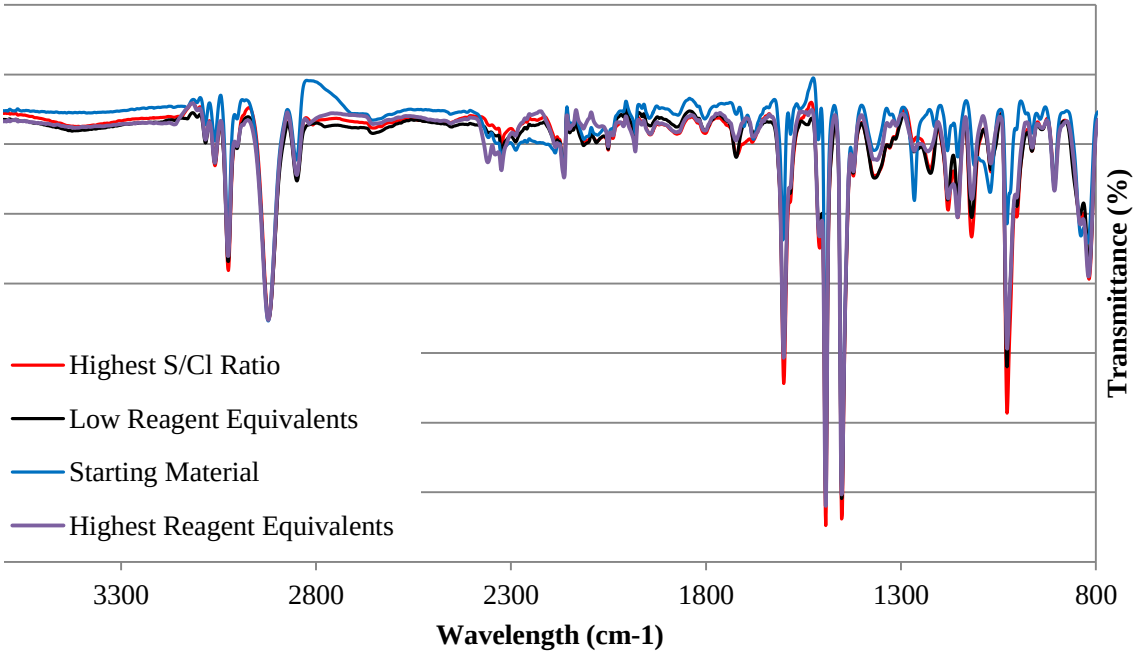

Figure 12: ATR-FTIR Spectra

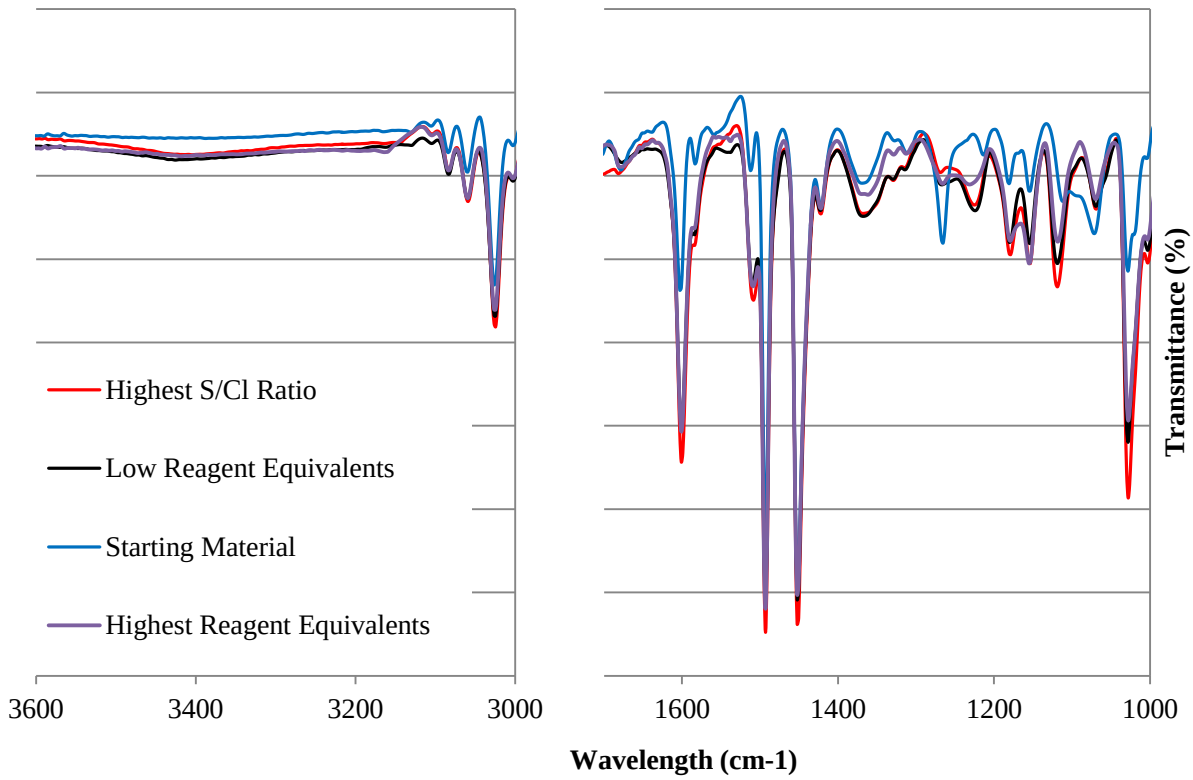

Figure 13: Areas of Importance in FTIR Spectra

2.3 Hydrolysis of Cellobiose

Based on conventional thinking of catalysis, the hypothesis for the hydrolysis of cellobiose was that by increasing the density of acid sites, the catalytic activity would increase. We hypothesized that the catalyst with the highest S/Cl ratio and the highest amount of sites would produce the most glucose. Figure 14 shows the hydrolysis of cellobiose into glucose. Cellobiose is a dimer of glucose joined by β, 1-4 glycosidic bonds, the same bond as cellulose, making it a good molecule to test catalytic activity of cellulose. The hydrolysis reactions were conducted using equal amounts of catalyst and cellobiose. After the reactions were complete they were quenched with water and diluted. The diluted samples were then run on high pressure liquid chromatography (HPLC) to detect cellobiose and glucose as well as isomerization products.

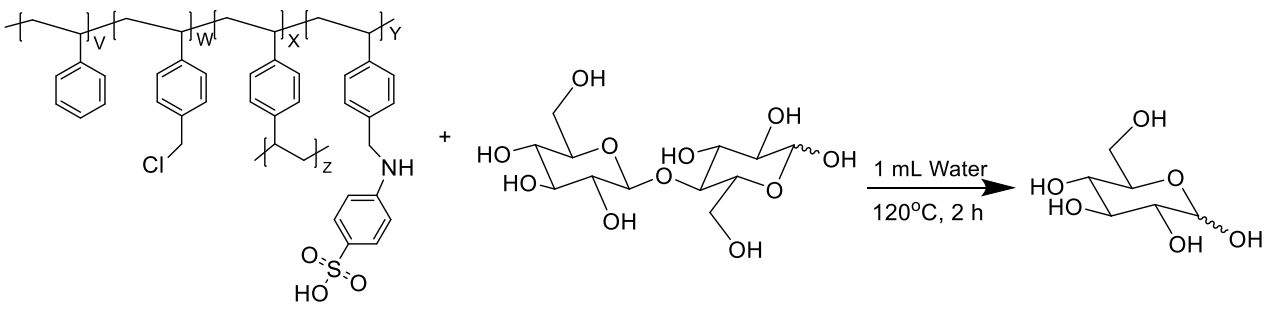

Figure 14: Hydrolysis Reaction of Cellobiose

Figure 15 shows the HPLC spectra of five catalytic hydrolyses of cellobiose. The hydrolysis of only cellobiose and no catalyst showed almost no glucose formed. Figures Figure 17 and Figure 17 show the percent yield of glucose from some catalysts. The catalyst with the highest site density and the lowest sulfur to chlorine ratio yielded the highest amount of glucose. Overall, the data seems fairly unreliable and hard to reproduce. Some error most likely occurred resulting in a high glucose yield produced by using solely the low density resin as a catalyst, and showed a higher result than expected. In general, the data does suggest that a higher amount of total sites and a lower amount of acidic sites has the highest catalytic activity. This is contrary to our hypothesis and the conventional theory of catalysis. This result is most likely due to the high amount of chlorine on the surface of the catalyst disrupting the inter- and intra-molecular bonds of cellobiose. The catalytic activity study indicates that binding sites are more important than cleaving sites. Most likely, there is an optimal ratio of S/Cl on the catalyst to yield the highest conversion. Our data indicates that this optimum S/Cl ratio is lower than the high site density catalyst we have produced.

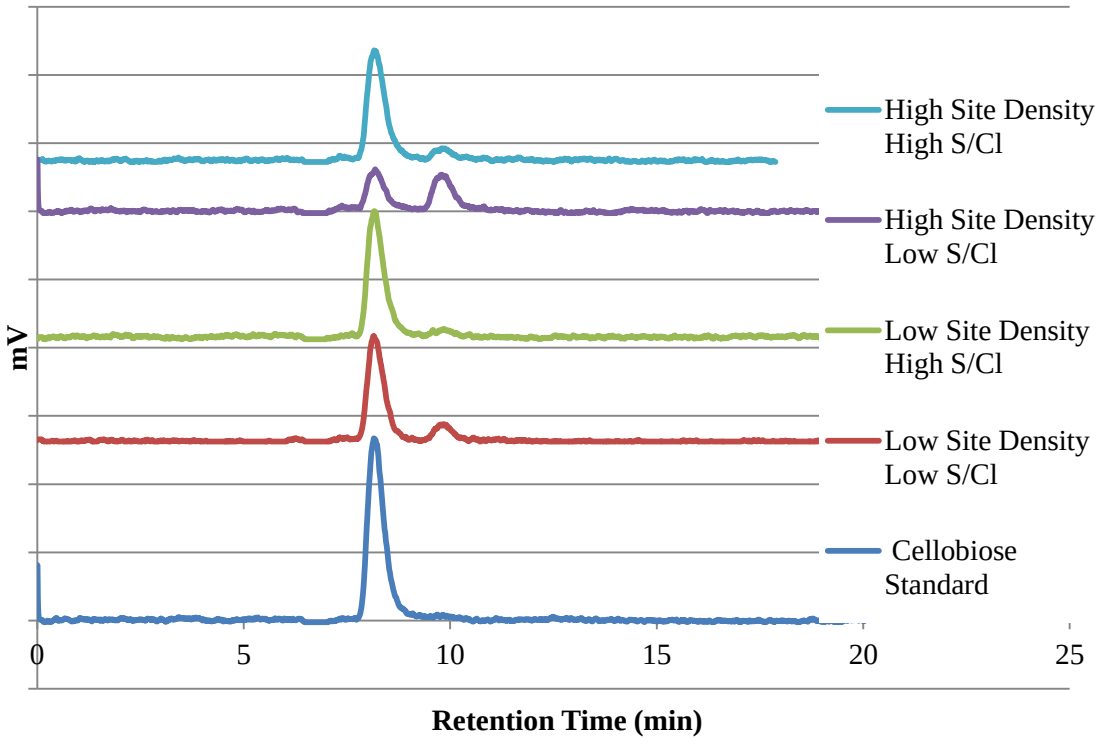

Figure 15: HPLC Spectra after Cellobiose Hydrolysis

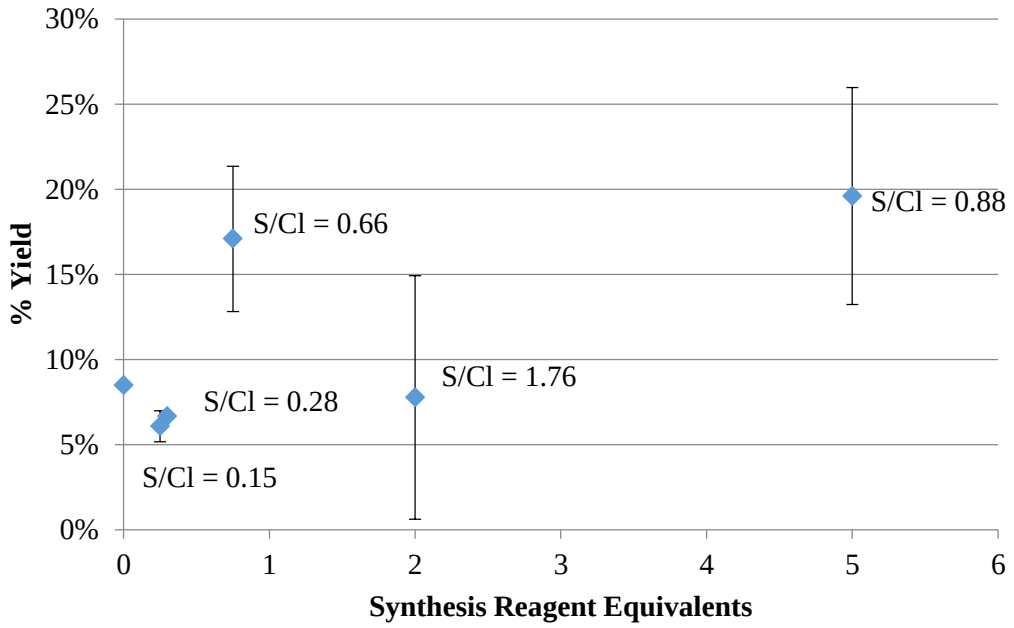

Figure 16: Percent Yield of Glucose from Cellobiose Hydrolysis with Low Site Density Catalysts

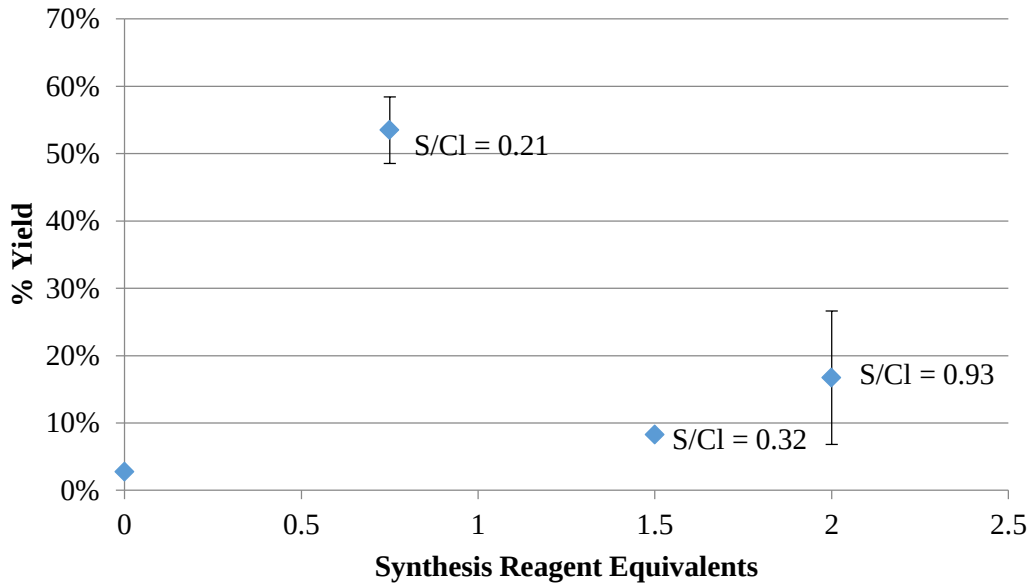

Figure 17: Percent Yield of Glucose from Cellobiose Hydrolysis with High Site Density Catalysts

2.3.1 Total Reflection X-Ray Fluorescence (TXRF) Spectroscopy Analysis of the Catalysts after Hydrolysis

After the catalysts underwent hydrolysis with cellobiose, they were filtered from the solution. Presumably, the catalysts should not have changed their chemical formula in terms of chlorine and sulfur. We wanted to run the catalysts through TXRF to see if there were any unpredicted reactions occurring (Figure 18). Only six catalysts were tested due to time constraints. In general the difference in S/Cl between the catalysts before and after hydrolysis is minimal and most likely due to small amounts of error. The catalysts that had 5 equivalents of sulfanilic acid added during synthesis, however, shows a significant increase in S/Cl after hydrolysis. Since it did not gain sulfur during hydrolysis; it lost chlorine during hydrolysis. This catalyst was to the right of the maximum S/Cl found at four equivalents of sulfanilic acid added to the catalyst synthesis, and the only catalyst of this type tested in hydrolysis of cellobiose. More catalysts needed to be tested in order to make any conclusions on this data.

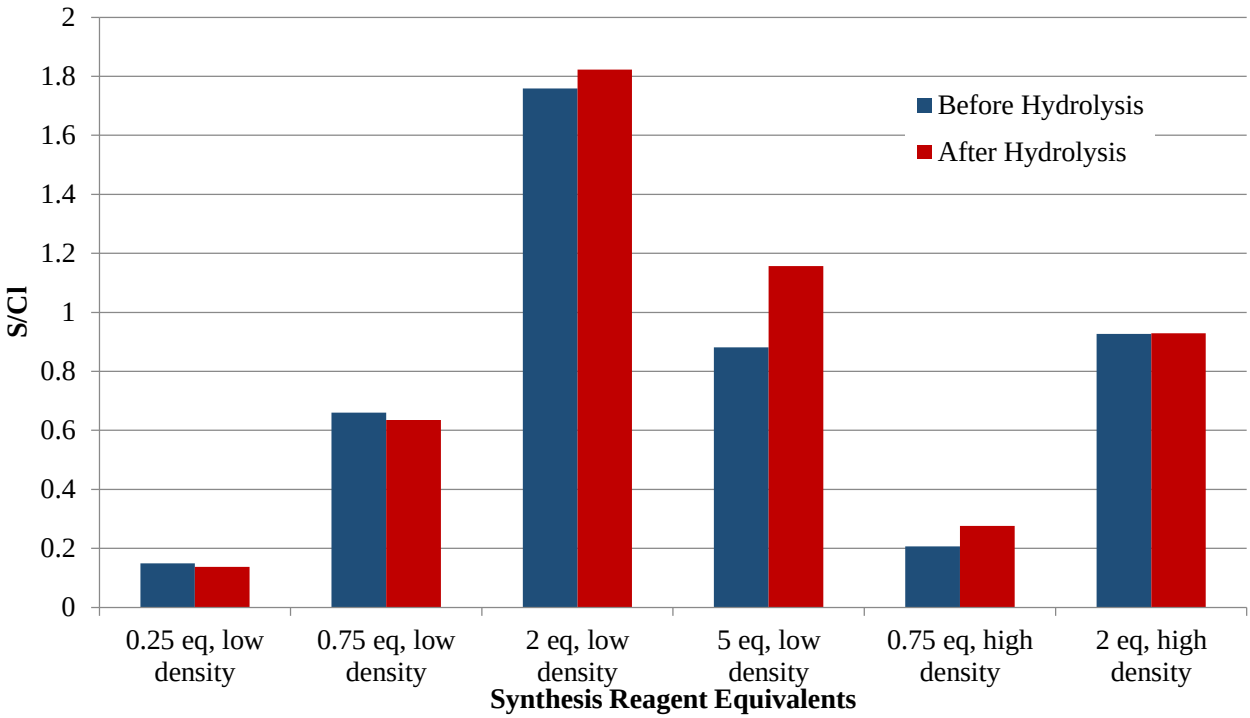

Figure 18: TXRF Analysis Before and After Hydrolysis

3 Future Directions

An area to be further investigated is the importance of total sites on the catalyst. As shown in the small sample size so far, a higher total amount of sites results in a higher conversion to glucose. Investigation of catalysts would allow us to compare a variety of catalysts with the same sulfur to chlorine ratio, and only varying by the amount of total sites. This could determine the optimum amount of total sites for the cellulase mimetic catalyst. Substrates can be commercially bought with chlorine content varying from 0.8 – 5.5 mmol/g. It could also be possible to synthesize starting material with higher amounts of total sites.

Another area to investigate in the future is the importance of DMF in synthesis. By varying the amount of DMF used in synthesis, the sulfur to chlorine ratio in the catalyst could change. Lowering the amount of DMF would also be more economically feasible and generate less waste. One way to determine a better solvent would be to conduct a swelling study. The solvent that swells the polymer the most would be the best option for a solvent during synthesis.

Further into the future, alternate binding and cleaving sites could be used. Different binding and cleaving sites could improve the depolymerization and hydrolysis. This would provide insight on creating the ideal catalyst to convert cellulose to glucose.

4 Experimental Section

4.1 General Procedures: Techniques, Solvents and Chemicals

All reactions and syntheses were performed in air. Solvents used were commercially bought. Reagents used were purchased from TCI America and Sigma Aldrich. Chloromethyl Polystyrene (100 mesh) with 1.2, or 2.4 mmol chlorine per gram resin was dried at 105 °C overnight prior to use. Reagents were purchased and used without additional purification.

4.1.1 Small Batch Synthesis of Sulfonated Chloromethyl Polystyrene (CP-SO3H) [26]

The synthesis of CP-SO_3H is shown in Scheme 1. The oven-dried Chloromethyl Polystyrene resin (500 mg, 0.6 mmol Cl) and DMF (8.3 mL) were added to a 20 mL scintillation vial, and sealed with a Teflon-sealed vial cap. The vial was stirred at 120 °C for 30 minutes on a hotplate, as instructed by literature. The reaction was taken off of the hotplate and varying amounts of sulfanilic acid were added (Table 2). The reactions were placed on the hotplate at 120 °C for 48 hours. After the reactions were complete, the vials were cooled to room temperature. The resin was recovered by filtration (with 10 µm nylon mesh membrane), washed with 30 mL of ethanol and 60 mL of water. The resin was then dried in an oven at 105 °C overnight before characterization and hydrolysis.

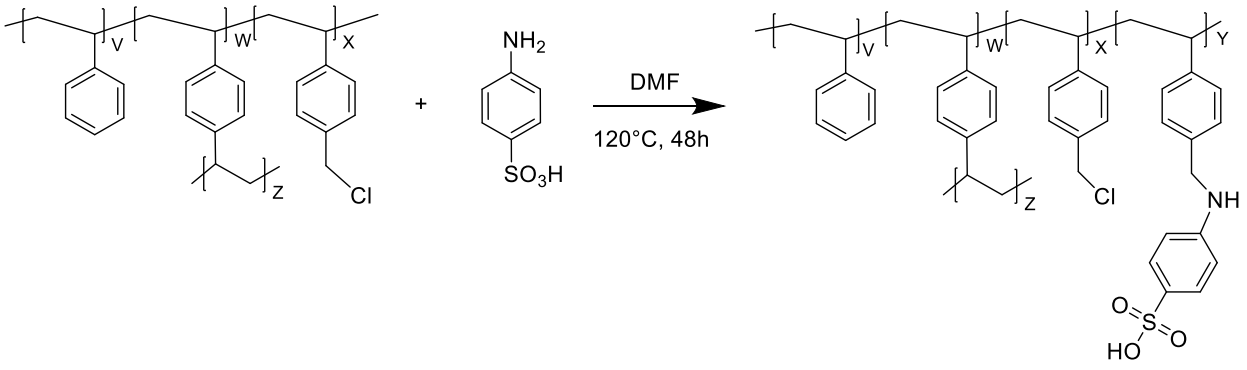

Scheme 1: General Synthesis Procedure

Table 2: Weights of Catalysts through Small Batch Synthesis. Conditions: CP Resin (500 mg, 0.6 mmol Cl, 1 eq.), DMF (8.3 mL), Sulfanilic Acid (varying amounts), 120 °C. The Sulfur to Chlorine ratio was determined through TXRF analysis. The ratio is the average of two samples from the same batch of catalyst. The reported error is the standard deviation of the two analyses.

Entry	Density of Cl in Substrate	mmol Cl	Reagent Equivalents	Amount of Catalyst (g)	S/Cl
1AJW95A	1.2 mmol/g	0.6	0.5	N/A	0.587 ± 0.00005
1AJW95B	1.2 mmol/g	0.6	0.75	N/A	0.9587 ± 0.0001
1AJW95C	1.2 mmol/g	0.6	1	N/A	1.1884 ± 0.0006
1AJW95D	1.2 mmol/g	0.6	1.25	N/A	1.6926 ± 0.0003
1AJW99A	1.2 mmol/g	0.6	2	N/A	1.995 ± 0.001
1AJW99B	1.2 mmol/g	0.6	5	N/A	2.365 ± 0.0006
1AJW99C	1.2 mmol/g	0.6	2.25	N/A	1.835 ± 0.0002
1AJW99D	1.2 mmol/g	0.6	2.5	N/A	1.89 ± 0
1AJW99E	1.2 mmol/g	0.6	4	N/A	2.445 ± 0.011
2AJW1A	1.2 mmol/g	0.6	0.25	0.4869	0.1357 ± 0.0004
2AJW1B	1.2 mmol/g	0.6	3.25	0.4934	2.3116 ± 0.00025
2AJW1C	1.2 mmol/g	0.6	4.5	0.4993	2.3632 ± 0.0687
2AJW1D	1.2 mmol/g	0.6	6	0.5126	1.9946 ± 0.014
2AJW18A	1.2 mmol/g	0.6	10	N/A	1.3332 ± 0.0017

4.1.2 Large Batch Synthesis of Sulfonated Chloromethyl Polystyrene (CP-SO3H) [26]

The synthesis of CP-SO_3H is shown in Scheme 1. The oven-dried Chloromethyl Polystyrene resin (3 g, 3.6 or 7.2 mmol Cl) and DMF (50 mL) were added to a 100 mL round-bottom flask, and sealed with a cap and clamp. The flask was stirred at 120 °C for 30 minutes in an oil bath, as instructed by literature. The reaction was taken off of the hotplate and varying amounts of sulfanilic acid were added (Table 3). The reactions were placed in the oil bath at 120 °C for 48 hours. After the reaction, the flasks were cooled to room temperature. The catalyst was recovered by filtration (with 10 µm nylon mesh membrane) followed by washing with 100 mL of ethanol and 200 mL of water. The catalyst was then dried in an oven at 105 °C overnight before characterization and hydrolysis.

Table 3: Weight of Catalysts through Large Batch Synthesis Conditions: CP Resin (3 g, 3.6 or 7.2 mmol Cl, 1 eq.), DMF (50 mL), Sulfanilic Acid (varying amounts), 120 °C. The Sulfur to Chlorine ratio was determined through TXRF analysis. The ratio is the average of two samples from the same batch of catalyst. The reported error is the standard deviation of the two analyses.

Entry	Density of Cl in Substrate	mmol Cl	Reagent Equivalents	Amount of Catalyst (g)	S/Cl
2AJW9A	1.2 mmol/g	3.6	0.75	2.994	0.6603 ± 0.0007
2AJW9B	1.2 mmol/g	3.6	2	3.004	1.759 ± 0
2AJW11A	2.4 mmol/g	7.2	0.75	2.9888	0.2068 ± 0.0007
2AJW11B	2.4 mmol/g	7.2	2	3.0329	0.9266 ± 0.0001
2AJW13A	1.2 mmol/g	3.6	1.5	3.067	1.7127 ± 0.114
2AJW13B	1.2 mmol/g	3.6	3	3.1206	3.4452 ± 0.0182
2AJW15A	1.2 mmol/g	3.6	5	3.1053	0.8818 ± 0
2AJW15B	1.2 mmol/g	3.6	0.25	2.9662	0.1496 ± 0
2AJW17A	2.4 mmol/g	7.2	4	2.5000	0.0437 ± 0
2AJW17B	2.4 mmol/g	7.2	3	3.4782	0.4885
2AJW19A	1.2 mmol/g	3.6	4	3.0858	0.7087 ± 0.0036
2AJW19B	1.2 mmol/g	3.6	0.3	2.9029	0.2785
2AJW20A	2.4 mmol/g	7.2	1.5	2.6320	0.3173

4.1.3 Hydrolysis of Cellobiose

250 mg of both CP-SO_3H and cellobiose was added to a 15 mL pressure vessel, along with 1.0 mL of water and a stirbar. The vessels were put in an oil bath at 120 °C and well stirred for two hours. After the reaction time was completed, the vessels were quenched using cool water. The reactions were filtered and diluted with DI water to 15 g each. Next, a 0.5 g aliquot was taken and diluted with 9.5 g of DI water. Finally, a 0.5 g aliquot of was added to 1.5 g of DI water. After dilution they were analyzed on HPLC using both visible light (to detect glucose and cellobiose) and ultra violet light (to detect isomerization products).

4.1.4 Acid Base Titration [30]

Acid base titrations were used to determine the acid loading of the CP-SO_3H. Varying amounts (0.5-1.5 g) of CP-SO_3H was added to 40 mL 0.05 M NaOH. The amount was

determined based on the S/Cl ratio of the catalysts. The samples were shaken for 24 hours. The solid was filtered out using 10 µm nylon mesh membrane. A 15 mL aliquot of the catalyst and 0.05 M NaOH solution was taken. 0.05 M HCl was titrated directly into this aliquot. The formula for determining the amount of moles of sulfonic acid on the catalysts through a back titration is (1).

$$n_{SO_3H} = [B]V_B - ([HCl]V_{HCl})\frac{V_B}{V_S} \qquad (1)$$

4.2 Analytical Methods

4.2.1 Fourier Transform Infrared (FTIR) Spectroscopy

FTIR spectra were recorded on a Bruker Vertex 70 with an Attenuated Total Reflection (ATR) sampling accessory. FTIR spectra were used to identify chemical bonds in the CP resin, CP-SO_3H, and sulfanilic acid. An example spectrum of catalyst 9 A can be seen below, Figure 19. All FTIR spectra can be found in the external file AJW on the server research.wpi.edu\emmertlab.

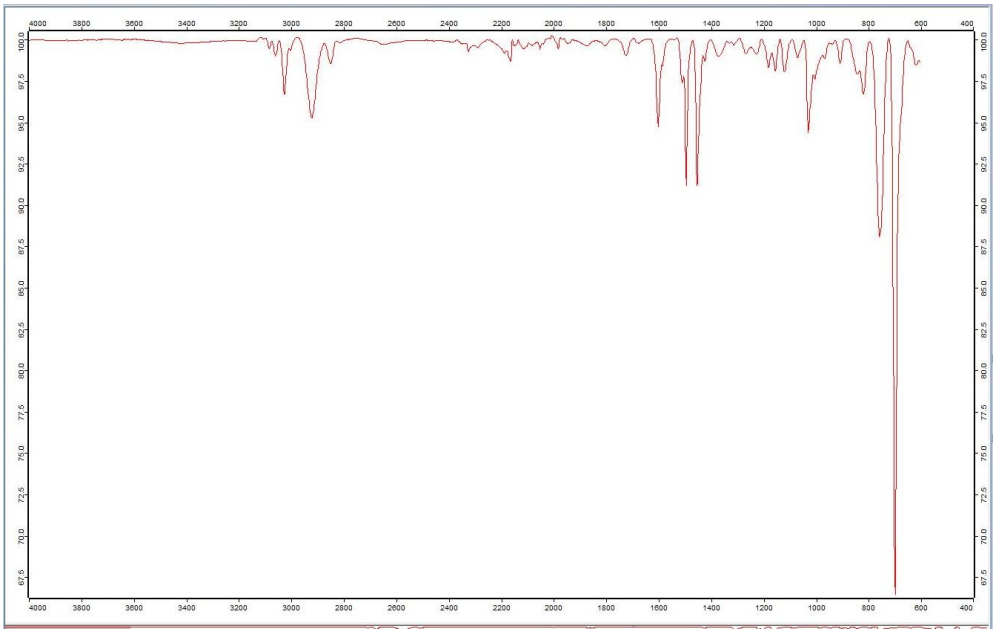

Figure 19: Sample ATR-FTIR spectrum

4.2.2 Total Reflection X-Ray Fluorescence (TXRF) Spectroscopy

TXRF spectra were recorded on a Bruker S2 Picofox. TXRF spectra were used to quantify the ratio of sulfur to chlorine in the CP-SO_3H. A sample TXRF spectrum of catalyst 20 A spectrum can be seen below, Figure 20. The Sulfur and Chlorine region of all TXRF spectra taken can be seen in Figure 21. All TXRF spectra can be found in the external file AJW on the server research.wpi.edu\emmertlab.

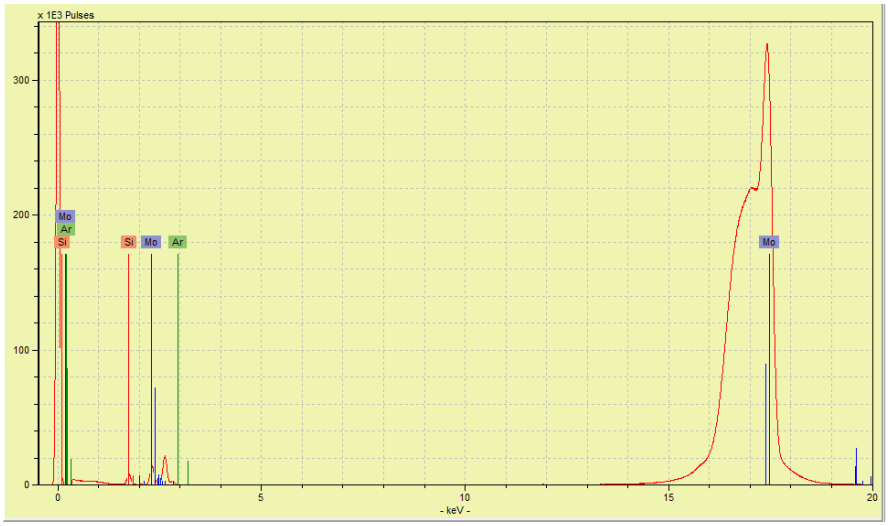

Figure 20: Sample TXRF Spectrum

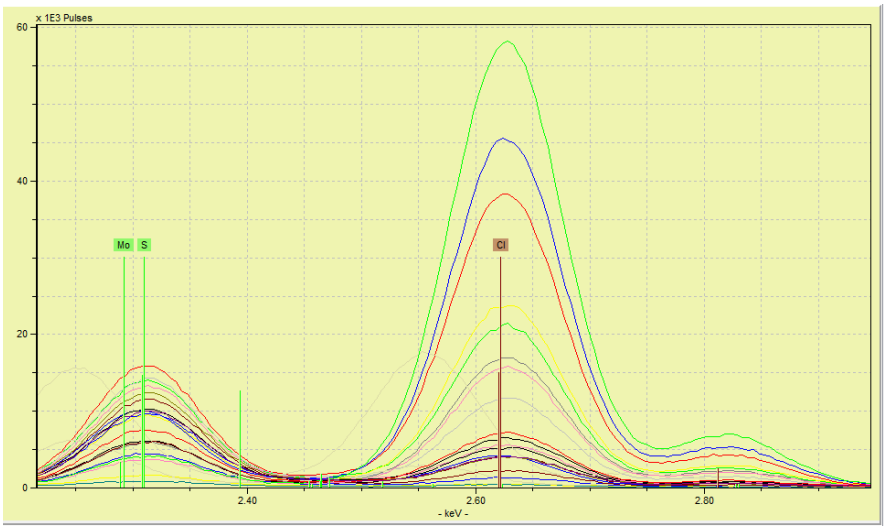

Figure 21: Sulfur and Chlorine Region of TXRF Spectra

4.2.5 High Pressure Liquid Chromatography (HPLC)

The HPLC column is a Phenomenex Rezex ROA-Organic Acid H+ (8%), size 300x7.8 mm. The visible light detector is a Sedere, Sedex 75 light scattering detector, T=65°C, gain=10, P=2.1 bar. The UV-vis detector is a Shimadzu SPD-10A, 285nm light. The mobile phase used is 0.00035 M sulfuric acid. The hydrolysis solutions were first quenched and diluted with water to 15 g total. A 0.5 g aliquot of this solution was then diluted with 9.5 g of water. A 0.5 g aliquot of this solution was then diluted with 1.5 g of water. This solution was then filtered using a 0.2 µm nylon filter before being analyzed in the HPLC. A sample UV-vis spectrum of hydrolysis solution 15 A can be seen below, Figure 22. A sample visible light spectrum of hydrolysis solution 15 A can be seen below, Figure 23.

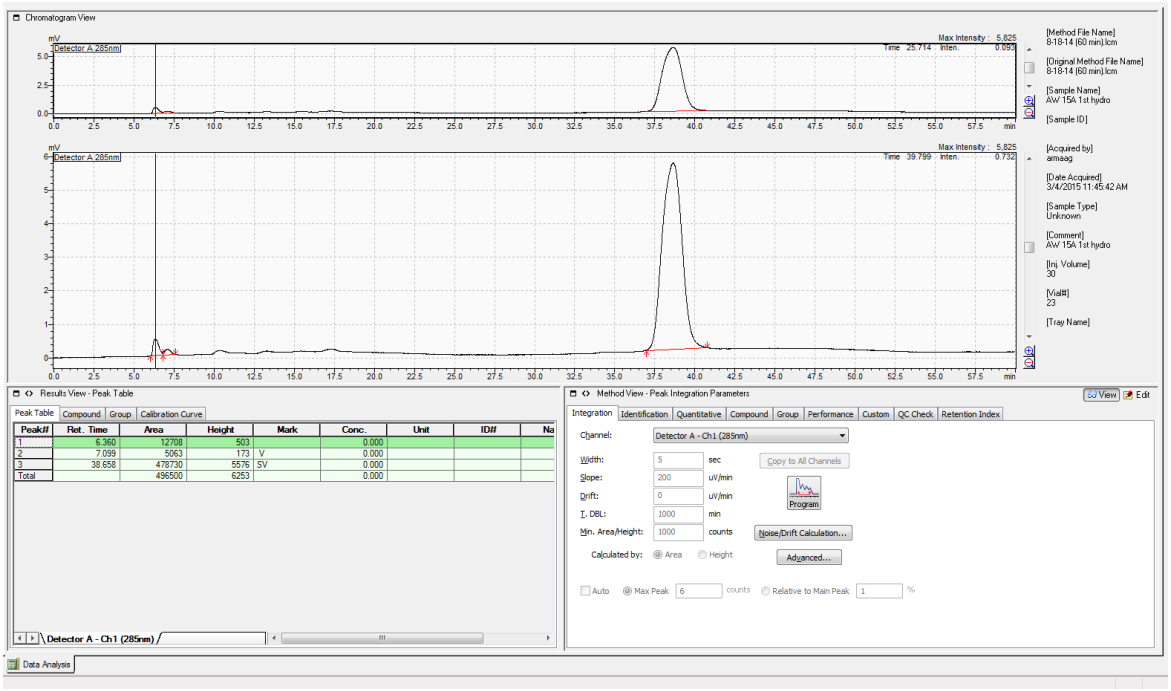

Figure 22: Sample UV-Vis HPLC Spectrum

Figure 23: Sample Visible Light HPLC Spectrum

Works Cited

1. Biomass Explained. http://www.eia.gov/energyexplained/index.cfm?page=biomass_home.

2. Kobayashi, H.; Fukuoka, A. Synthesis and Utilisation of Sugar Compounds Derived from Lignocellulosic Biomass. *Green Chem.* **2013,** *15,* 1740.

3. Huang, Y.-B.; Yao, F. Hydrolysis of Cellulose to Glucose by Solid Acid Catalysts. *Green Chem.* **2013,** 1095-1111.

4. Bornscheuer, U.; Buchholz, K.; Seibel, J. Enzymatic Degradation of (Ligno)cellulose. *Angew Chemie* **2014,** 2-20.

5. Hook, M.; Tang, X. Depletion of Fossil Fuels and Anthropogenic Climate Change - A Review. *Energy Policy* **2013,** *52,* 797-809.

6. Balan, V. Current Challenges in Commercially Producing Biofuels from Lignocellulosic Biomass. *ISRN Biotechnology* **2014**.

7. McKendry, P. Energy Production from Biomass (PArt 1): Overview of Biomass. *Bioresource Technology* **2002,** *83* (1), 37-46.

8. Perlack, R. D.; Wright, L. L.; Turhollow, A. F.; Graham, R. L.; Stokes, B. J.; Erbach, D. C. *Biomass as Feedstock for a Bioenergy and Bioproducts Industry: The Technical Feasibility of a Billion-Ton Annual Supply;* U.S. Department of Energy & U.S. Department of Agriculture: Oak Ridge, TN, 2005.

9. Costa, R. C.; Sodre, J. R. Hydrous Ethanol Vs. Gasoline-Ethanol Blend: Engine Performance and Emissions. *Fuel* **2010,** *89* (12), 287-293.

10. Sales, C. M.; R., S. J. Cold Start Characteristics of an Ethanol-Fuelled Engine with Heatd Intake Air and Fuel. *Applied Themal Engineering* **2012,** *40,* 198-201.

11. Luque, R.; Herrero-Davila, L.; Campelo, J. M.; Clark, J. M.; Hdalgo, J. M.; Luna, D.; Marinas, J. M.; Romero, A. A. Biofuels: a technological perspective. *Energy Environ. Sci.* **2008,** *1* (5), 542–564.

12. Metzger, M. J.; Glasser, B. J.; Patel, B.; Fox, J.; Sempuga, B. C.; Hildebrandt, D.; Glasser, D. Liquid Fuels from Alternative Carbon Sources Minimizing Carbon Dioxide Emissions. *AIChE Journal* **2013,** *59* (6), 2062-2078.

13. Gray, K. A.; Zhao, L.; Emptage, M. Bioethanol. *Current Opinion in Chemical Biology* **2006,** *10* (2), 141-146.

14. Buléon, A.; Colonna, P.; Planchot, V.; Ball, S. Starch granules: structure and biosynthesis. *International Journal of Biological Macromolecules* **1998,** *23* (2), 85-112.

15. Wang, N. S. Starch Hydrolysis by Amylase. http://www.eng.umd.edu/~nsw/ench485/lab5.htm (accessed Jan 13, 2015).

16. Krempels, D. M. The Molecules that Make Plant Cells.Different. http://www.bio.miami.edu/ (accessed March 8, 2015).

17. Schnepf, R.; Yacobucci, B. D. *Renewable Fuel Standard;* Congressional Report; Congressional Research Services: Washington DC, 2013.

18. Sims, R. E. H.; Mabee, W.; Saddler, J. N.; Taylor, M. An overview of second generation biofuel technologies.. *Bioresource Technology* **2010,** *101* (6), 1570-1580.

19. Doornbosch, R.; Steenblik, R. Biofuels: Is the Cure Worse then the Disease? *Organisation de Coopération et de Développement Economiques* , Paris, 2007; pp 0-54.

20. Stephen, J. D.; Mabee, W. E.; Saddler, J. N. Will Second-Generation Ethanol be able to Compete with First-Generation Ethanol? Opportunities for Cost. *Biofuels, Bioprod. Bioref.* **2011**.

21. Pang, Q.; Wang, L.; Yang, H.; Jia, L.; Pan, X.; Qiu, C. Cellulose-derived carbon bearing –Cl and –SO3H groups as a highly selective catalyst for the hydrolysis of cellulose to glucose. *RSC Adv.* **2014,** *4*, 41212.

22. Lu, J.; Reye, J.; Banerjee, S. Temperature Dependance of Cellulase Hydrolysis of Paper Fiber. *Biomass and Bioenergy* **2010,** *34* (12), 1973-1977.

23. Ado, Y.; Asada, Y.; Benemann, J. R.; Kishimoto, M.; Miyake, J.; Miyamoto, K.; Nishio, N. Renewable Biological Systems for Alternative Sustainable Energy Production. *Food and Agriculture Organization of the United Nations,* Osaka, Japan, 1997.

24. Wilson, D. B. Cellulases and Biofuels. *Current Opinion in Biotechnology* **2009,** *20* (3), 295-299.

25. Acharva, S.; Chaudhary, A. Bioprospecting Thermophiles for Cellulase Production: a review. *Braz. J. Microbiol.* **2012,** *43* (3), 844-856.

26. Shuai, L.; Xuejun, P. Hydrolysis of Cellulose by Cellulase-Mimetic Solid Catalyst. *Energy Environ. Sci.* **2012,** 6889-6894.

27. Dutta, S. Catalytic Materials that Improve Selectivity of Biomass Conversions. *RSC Adv.* **2012,** *2,* 12575-12593.

28. Campbell, A. M. Beta-1,4-Endoglucanase. http://www.bio.davidson.edu/ (accessed March 9, 2015).

29. Deng, W.; Lobo, R.; Setthapun, W.; Christensen, S. T.; Elam, J. W.; Marshall, C. L. Oxidative Hydrolysis of Cellobiose to Glucose. *Biotechnology and Bioprocess Engineering* **2011,** *16* (6), 1214-1222.

30. Goertzen, S. L.; Thériault, K. D.; Oickle, A. M.; Tarasuk, A. C.; Andreas, H. A. Standardization of the Boehm titration. Part I. CO2 expulsion and endpoint determination. *Carbon* **2010,** *48* (4), 1252–1261.

31. Kumar, P.; Barrett, D. M.; Delwiche, M. J.; Stroeve, P. Methods of Pretreatment of Lignocellulosic Biomass for Efficient Hydrolysis and Biofuel Production. *Ind. Eng. Chem. Res.* **2009,** 3713-3729.

32. Petroleum & Other Liquids, 2014. U.S. Energy Information Administration. http://www.eia.gov/dnav/pet/hist/LeafHandler.ashx?n=pet&s=emm_epm0_pte_nus_dpg&f=w

(accessed Oct 27, 2014).

33. Agency, U. S. E. P. EPA Lifecycle Analysis of Greenhouse Gas Emissions from Renewable Fuels, 2009. National Service Center for Environmental Publications. nepis.epa.gov (accessed Dec 20, 2014).

34. Dutta, S. Catalytic Materials that Improve selectivity of Biomass Conversions. *RSC Advances* **2004**.